

A MEMS Nanopositioner with Thermal Actuator and On-chip Thermal Sensor

Y. Zhu, S. O. R. Moheimani, M. R. Yuce

School of Electrical Engineering and Computer Science, The University of Newcastle
University Drive, NSW, 2308, Australia

Email: {yong.zhu, reza.moheimani, mehmet.yuce}@newcastle.edu.au

Abstract— This paper describes the design of a micromachined nanopositioner with electrothermal actuation and sensing capabilities in a single silicon chip. The positioner has a dynamic range of 14.4 μm with a differential sensing scheme. At 6-V dc bias voltage, the position sensors have a power consumption of 120 mW, and a sensitivity of 0.27 mV/nm. The open-loop bandwidth is 101 Hz and the phase delay from 1 Hz to 51.2 kHz is 169°. The on-chip displacement sensing enables a feedback control capability.

I. INTRODUCTION

High precision nanopositioners have been used extensively in many applications such as scanning probe microscopy (SPM) [1], atomic force microscopy (AFM) [2], and emerging ultrahigh density probe storage system [3,4]. Closed-loop feedback control of the positioners is highly desirable if a high degree of displacement precision is required, and such a control system needs an accurate source of position information [5]. However, in experimental MEMS nanopositioners, the in-plane movements are often measured by laser reflectance microscopes [6, 7] or optical microscopes [8], making the footprint of the whole system fairly large. There are few exceptions in the literature, for example, an embedded on-chip capacitive displacement sensor was integrated in a thermally actuated positioner in [9]. Nevertheless, a complex fabrication process was required for electrical insulation between electrical heating and sensing circuits. Recently, a novel thermal sensing scheme has been used in a probe-based storage device [10]. Micro-heaters were used to measure the motion of a MEMS micro-scanner with resolution of less than 1 nm. Compared to comb capacitive sensing, thermal sensing is more compact and can be easily integrated with actuators. In [11, 12], off-chip electromagnetic coil actuators were adopted for scanner actuation, and a complex mass-balanced structure was designed for vibration resistance purposes.

In this work, a novel electrothermal position sensor is integrated with an electrothermal actuator in the same MEMS chip without the need for inclusion of extra electrical insulation fabrication process [9], or assembling two chips as in [11]. Compared to other MEMS actuation mechanisms, the thermal actuators have advantages of low voltage operation,

large forces, and a high vibration resistance due to their stiff structures [13]. A MEMS device with integrated electrothermal actuation and sensing has been micro-fabricated in a bulk silicon process. Measurement results show that the positioner has a dynamic range of 14.4 μm . At 6-V dc bias voltage, the position sensors have a power consumption of 120 mW, and a sensitivity of 0.27 mV/nm. The open-loop bandwidth is 101 Hz and the phase delay from 1 Hz to 51.2 kHz is 169°.

II. DESIGN

The conceptual schematic view of the sensing part of the nanopositioner is presented in Fig.1. The position sensors are two beam-shaped resistive heaters made from doped silicon. Application of a fixed dc voltage across the heaters results in a current passing through them, thereby heating the beams. As a heat sink, a rectangular plate is placed beside the beam heaters with a 2 μm air gap.

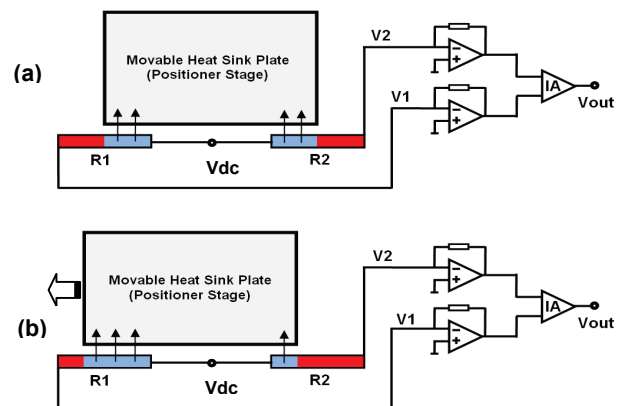


Figure 1. Schematic diagram of the thermal position sensor with a differential amplifier circuit: (a) Initial position; (b) After actuation.

Before applying voltage on the actuator, the positioner stage is at the initial rest position (Fig.1a), where the two edges of the positioner are precisely aligned with the middle the two thermal resistive sensors R1 and R2. The sensors are biased by a dc voltage source V_{dc} , and the heat generated in the resistive heater is conducted through the air to the heat

sink plate (positioner stage). As the plate is centered between the two thermal sensors, the heat fluxes out of the sensors are identical, thereby equaling the temperature and resistance of the sensors. After applying a voltage on the actuator beams, the positioner stage is displaced towards left, the heat flux associated with the sensor on the left increases, while that of the sensor on the right decreases, resulting in a decrease in the resistance of the left sensor (R1), and an increase in resistance of the right sensor (R2). Thus, the displacement information of the positioner stage can be detected by measuring the resistance difference between the two sensors. The differential changes of the resistance result in current variations in the beam resistors, and the currents are converted to an output voltage using the trans-impedance amplifiers and an instrumentation amplifier, as illustrated in Fig.1. To suppress the common-mode noise, the gains of these two trans-impedance amplifiers must be well matched. Employing the differential topology allows the sensor output to be immune from undesirable drift effects due to changes in ambient temperature or aging effects.

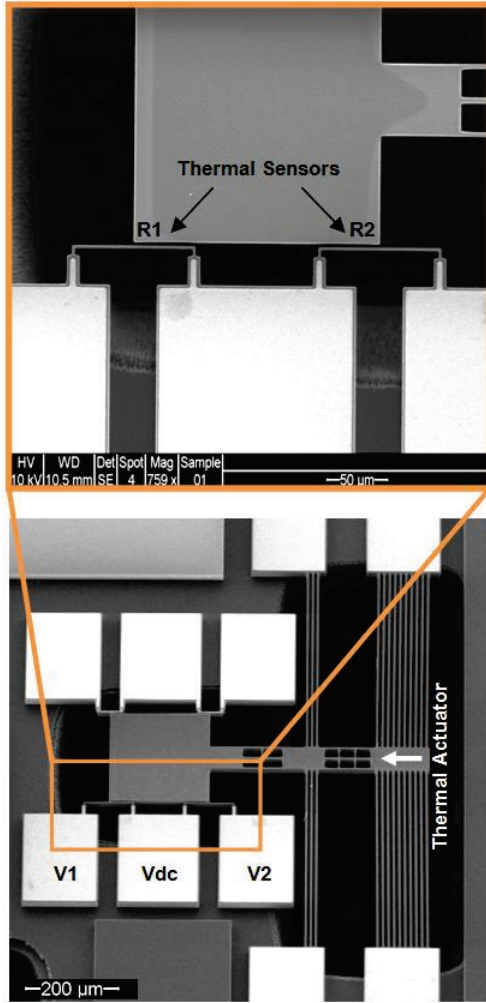


Figure 2. SEM images of the micromachined nanopositioner.

The image of the whole device and a section of it taken under a Scanning Electron Microscope (SEM) are provided in Fig.2.

The positioner stage is actuated by a chevron thermal actuator, as illustrated in Fig.2. Compared to other actuation methods, the thermal actuators are simple to implement, operate at low voltage, and provide large forces. Due to the stiffness of the structures, no complex mass-balanced structures are needed for vibration resistance purposes, as proposed in [12]. The chevron thermal actuator has two pairs of thin hot arms at a small angle with respect to each other as shown in Fig.2, and the dimensions are listed in Table I. The chevron actuator's operating voltage range is typically 0 to 15 V, depending on the geometry. The displacement is proportional to V^2 , and the maximum displacement is limited by buckling of the hot arms at high temperatures (>700 °C) [7].

To reduce the thermal coupling effects from the thermal actuators to thermal sensors, a number of holes were made in the centre shuttle between actuators and the heat sink plate. The holes are expected to improve the thermal convection, thereby thermally insulating the heat sink plate from actuators. The suspension beams help the insulation as well, because the heat can transfer to the substrate through the suspension beams and its anchors.

Table I summarizes the device design parameters and measured beam resistance.

TABLE I
GEOMETRIC AND MATERIAL PROPERTIES

Parameter	Value
Actuator beam width (μm)	5
Actuator beam length (μm)	2×400
Actuator beam angle (degree)	0.57
Actuator quantity (pair)	10
Suspension beam width (μm)	5
Suspension beam length (μm)	400
Actuator beam angle (degree)	0
Actuator quantity (pair)	3
Sensor beam width (μm)	2
Sensor beam length (μm)	100
The gap between sensor and heat sink plate (μm)	2
Heat sink plate dimension ($\mu\text{m} \times \mu\text{m}$)	200×200
Device thickness (μm)	25
Measured resistance of thermal sensor R1 at room temperature (Ω)	388.9
Measured resistance of thermal sensor R2 at room temperature (Ω)	391.6
Measured resistance of thermal actuator at room temperature (Ω)	116

III. FABRICATION

The device was micro-fabricated from single-crystal silicon using a commercial bulk silicon micromachining technology-SOIMUMP in MEMSCAP [14]. This process has a 25 μm thick silicon device layer and a minimum feature/gap of 2 μm . Fig.3 provides an illustrated summary of this fabrication process:

- 1) Surface metal pads are patterned on a highly doped n-type 25 μm silicon device layer to allow for ohmic contact.
- 2) Deep reactive ion etch (DRIE) from the front side of the wafer to define both the anchored and movable features of the structure.
- 3) A protective polyimide layer is applied to the front side.
- 4) A deep trench underneath the movable structures is created by etching through the substrate using DRIE.
- 5) The exposed buried oxide is removed using a wet HF etch.
- 6) The polyimide coat on the front side is removed by oxygen plasma, thereby allowing the movable structure to be fully released. Then a large contact metal pad is patterned on the substrate for electrical contact.

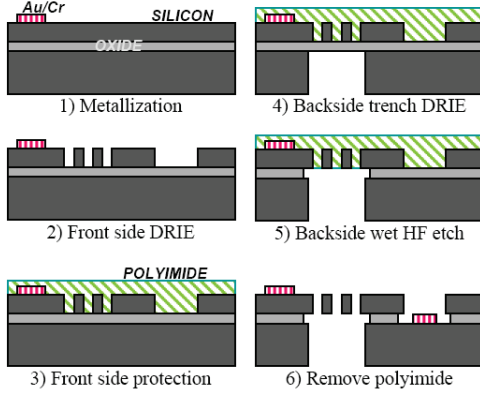


Figure 3. SOIMUMPs fabrication process through MEMSCAP

IV. EXPERIMENTAL RESULTS

The nanopositioner was calibrated using a PolytecTM Planar Motion Analyzer (PMA). Digital image capture and analysis methods were used to determine the displacement of the positioner stage.

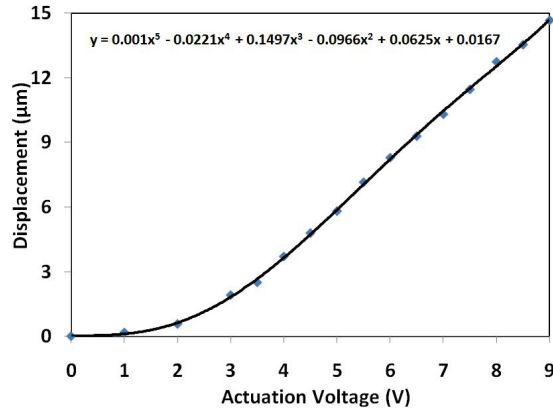


Figure 4. Experimental calibration results for the thermal actuator: actuation displacement versus actuation voltage.

The static actuation voltage vs. displacement results are shown in Fig.4. With the actuation voltage of 9 V, the thermal actuator can achieve a maximum displacement of 14.4 μm . Due to the nature of the thermal expansion, the actuator can only move forward in one direction after voltage application

from 0 V. However, the actuator can be biased to an initial position by a dc voltage, such that it can move forward or backward by increasing or decreasing the voltage. For instance, for a 10 μm travel range with bi-directional movement application, the actuator can be actuated by a 4.5-V dc voltage to the middle position (5 μm) of the desired range.

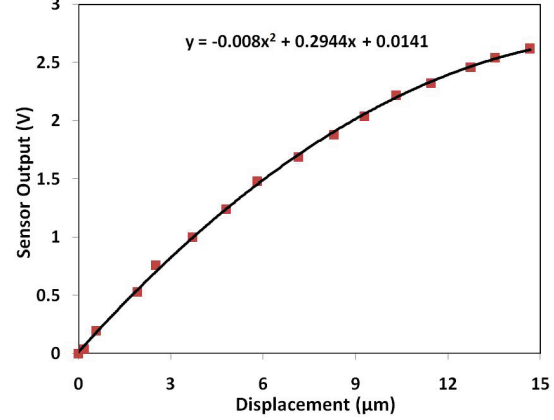


Figure 5. Experimental calibration results for the position sensor: instrumentation amplifier output versus actuation displacement.

At every actuation voltage, the instrumentation amplifier outputs were recorded for the calibration of the position sensors, as illustrated in Fig.5. The sensors were biased with 6-V dc voltage, and the instrumentation amplifier's gain was set at 90.3 V/V. At this bias voltage, the sensors have a power consumption of 120 mW, and the sensitivity is 0.27 mV/nm at a displacement range of about 6 μm . The sensitivity decreases when the displacement is more than 6 μm . A possible reason is that the temperature distribution is not even in the thermal sensor beams. Due to the heat loss in the anchor of the sensor beams, the middle of the beam is hotter than the two ends of the beam, which has been described in [15]. The experimental calibration results of the instrumentation amplifier output versus the actuation voltage are shown in Fig.6.

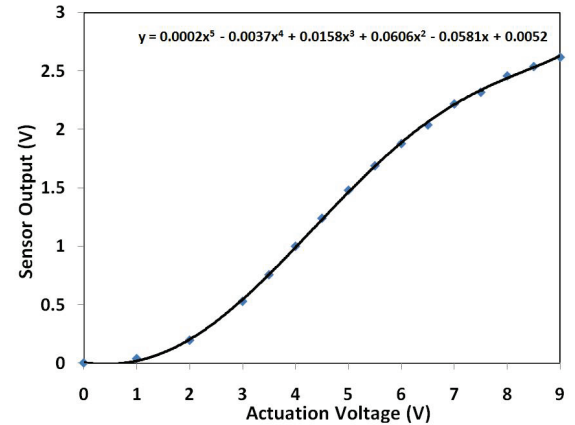


Figure 6. Experimental calibration results for the nanopositioner: instrumentation amplifier output versus actuation voltage.

The dynamic characterization was conducted using a HP35670A spectrum analyzer. A voltage of 4.5 V dc plus 1 V ac was applied to the actuator and swept sinusoidal measurements were obtained from 1 Hz to 51.2 kHz by the

on-chip thermal sensors. The frequency response illustrated in Fig. 7 shows the open-loop bandwidth of the positioner is 101Hz. The phase delay from 1 Hz to 51.2 kHz is 169°, which is caused by the heating and cooling time in the thermal beams in actuators and sensors.

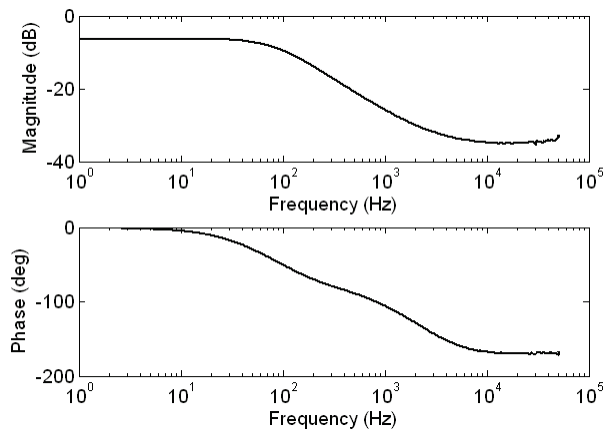


Figure 7. Experimental frequency response of the nanopositioner motion as measured by the on-chip thermal sensors.

V. CONCLUSION

A novel micromachined silicon nanopositioner with on-chip thermal actuator and sensor has been presented. A feedback controller can be designed and implemented to control the device by using the functions such as the actuation voltage versus displacement and displacement versus sensor output obtained in this work. The closed-loop feedback control of the developed positioner is currently under investigation. A 2DOF nanopositioner is currently under design, and will be reported in the future.

ACKNOWLEDGMENT

The authors would like to thank Dave Phelan from the school of Medical Sciences at University of Newcastle for his help on SEM images.

REFERENCES

- [1] G.Binning, and H.Rohrer, "The scanning tunneling microscope," *Sci.Am.*, vol.253, pp.50-56, 1986.
- [2] G.Binning, C.Quate, and C.Gerber, "Atomic force microscope," *Phys. Rev. Lett.*, vol.56, no.9, pp.930-933, 1986.
- [3] N.B.Hubbard, M.L.Culpepper, and L.L.Howell, "Actuators for micropositioners and nanopositioners," *Transactions of the ASME*, Vol.59 November 2006, pp.324-334.
- [4] A.Pantazi, M.A.Lantz, G.Cherubini, and H.Pozidis, and E.Eleftheriou, "A servomechanism for a micro-electro-mechanical-system-based scanning-probe data storage device," *Nanotechnology*, 15, pp.S612-S621, 2004
- [5] S.Devasia, E.Eleftheriou, and S.O.R.Moheimani, "A survey of control issues in nanopositioning," *IEEE Trans. on control systems technology*, vol. 15, no.5, 2007, pp.802-823
- [6] J.J. Gorman, Y-S. Kim, and N.G. Dagalakis, "Control of MEMS nanopositioners with nano-scale resolution," *Proceeding of IMECE2006*, Chicago, Illinois USA, November 5-10, 2006.
- [7] R.Hichey, D.Sameoto, T.Hubbard, and M.Kujath, "Time and frequency response of two-arm micromachined thermal actuators", *J.Micromech.Microeng.*, 13, (2003), pp.40-46.
- [8] Y.Sun, M.A.Greminger, D.P.Potasek, and B.J.Nelson, "A Visually Servoed MEMS Manipulator," *Experimental Robotics VIII*, Springer Berlin/Heidelberg, 2003, pp.255-264.
- [9] L.L. Chu, and Y.B. Gianchandani, "A micromachined 2D positioner with electrothermal actuation and sub-nanometer capacitive sensing", *J. Micromech. Microeng.*, 13 (2003), pp.279-285.
- [10] M.A.Lantz, G.K.Binning, M.Despont, and U.Drechsler, "A micromechanical thermal displacement sensor with nanometre resolution," *Nanotechnology*, 16 (2005), pp.1089-1094.
- [11] A.Sebastian, A.Pantazi, S.O.R. Moheimani, H.Pozidis, and E.Eleftheriou, "Achieving subnanometer precision in a MEMS-based storage device during self-servo write process," *IEEE Tran. on nanotechnology*, vol.7, no.5, 2008, pp.586-595
- [12] M.A.Lantz, H.E.Rothuizen, U.Drechsler, W.Haberle, and M.Despont, "A vibration resistant nanopositioner for mobile parallel-probe storage applications," *J. microelectromechanical systems*, vol.16, no1, 2007, pp.130-139.
- [13] V.Kaajakari, *Practical MEMS*. Small Gear Publishing, 2009.
- [14] http://www.memscap.com/en_mumps.html
- [15] U.Durig, "Fundamentals of micromechanical thermoelectric sensors," *Journal of Applied Physics*, 98,044906 (2005)